Synthesis of 2-Phenoxyacetic Acid Analogs for Evaluation of the Anti-inflammatory Potential and Subsequent *In Silico* Analysis

Md. Mofazzal Hossain[1,2], Bishyajit Kumar Biswas[1], and Sukumar Bepary[1*]

[1]*Department of Pharmacy, Jagannath University, 9–10 Chittaranjan Avenue, Dhaka 1100, Bangladesh*

[2]*Department of Pharmacy, University of Information Technology and Sciences, Holding 190, Road 5, Block J, Baridhara, Maddha Nayanagar, Vatara, Dhaka 1212, Bangladesh*

** **Corresponding author:***

tel: +880-1912 938593
email: sukumar@pharm.jnu.ac.bd

Received: May 8, 2024
Accepted: July 29, 2024

DOI: 10.22146/ijc.96015

Abstract: *Several 2-phenoxyacetic acid derivatives and their isosteres were synthesized in moderate to high yield (57–96%) for searching newer and safer alternatives to these existing anti-inflammatory agents. The compounds were characterized by ^{1}H-NMR, ^{13}C-NMR and HRMS. The synthesized compounds have been subjected to* in vitro *anti-inflammatory activity using egg albumin denaturation and human red blood cell membrane stabilization methods. The compounds were also evaluated for their anti-inflammatory activity in the mice model. The synthesized compounds were subsequently subjected to docking analysis. The* in vitro *pharmacokinetic properties were analyzed by applying the pkCSM software and drug-likeness was checked by using Lipinski's rule. Some synthesized esters and amides, like* ***SM61****,* ***SM81****,* ***SM82****,* ***SM83****,* ***SM91*** *and* ***SM101****, were significantly more powerful as anti-inflammatory agents. The efficacies were correlated with their orientations in the binding pocket of the cyclooxygenase enzyme. The encouraging* in vitro *and* in vivo *activities, the optimum pharmacokinetic profile, and good drug-likeness indicated that these scaffolds could be considered for future discovery of newer nonsteroidal anti-inflammatory drugs (NSAIDs).*

Keywords: *writhing; HRBC; docking; pharmacokinetic profile*

■ INTRODUCTION

Inflammation is a typical biological response resulting in the activation of immune and non-immune cells to protect the host from the damaging effects of toxins or various pathogens like bacteria and viruses. This bodily response eliminates pathogens and promotes tissue repair and recovery [1-2]. The degree and extent of the inflammatory responses are varied and can include local, metabolic, and neuroendocrinological responses. These changes may affect conserving metabolic energy by allocating more nutrients to the activated immune system [3-6]. If uncontrolled, these may lead to conditions known as "sickness behaviors" characterized by sadness, fatigue, reduced libido, lack of appetite, and hampered sleep. These may lead to various chronic disease states, including high blood pressure, insulin resistance, and dyslipidemia, which are critical for surviving in the long run [4-9].

The inflammatory responses, especially if untreated for a long time, may lead to a lot of non-communicable chronic diseases like ischemic heart disease, stroke, cancer, diabetes, non-alcoholic fatty liver disease, various autoimmune conditions, and neurodegenerative conditions. These are well known to affect social life. More alarming is that these are reported to account for more than 50% of all deaths worldwide in the present days, thereby appearing as the leading cause of death globally [10]. Additionally, a weakened immune system, due to persistent inflammations, makes the body more vulnerable to various types of infections, malignancies and poor response to immunizations [11].

Non-steroidal anti-inflammatory drugs (NSAIDs) comprise compounds with analgesic, antipyretic, and anti-inflammatory effects. The majority of these NSAIDs are acidic substances and need to be administered in higher dosing frequencies. Most patients

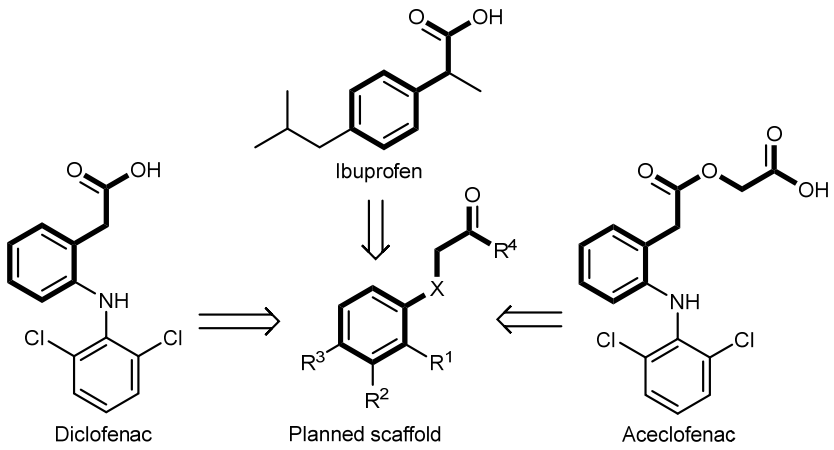

Fig 1. Proposed analogs

who use these medications are not recommended for long-term use because of their gastrointestinal, renal, and cardiovascular adverse effects [12]. Thus, there are continuous searches for developing newer drugs with greater efficacy but fewer side effects.

Aceclofenac, a cyclooxygenase inhibitor [13-14] has remarkable selectivity for COX-2 over COX-1 isoform when compared to commercialized medicines, such as ibuprofen and diclofenac. Thus, it has a preference for chronic inflammatory conditions, including lower back pain, osteoarthritis, extra-articular rheumatism, rheumatoid arthritis, and ankylosing spondylitis. These musculoskeletal conditions have been reported to be the leading causes of morbidity and disability, resulting in substantial healthcare costs and loss of working ability [15-16]. Even this new analog has a relatively better tolerability profile [17]. While looking for the structures of these agents, aceclofenac has an acid function that is a little far from the aromatic ring (Fig. 1). Thus, 2-phenoxyacetic acid analogs have been considered here to search for novel anti-inflammatory scaffolds. The analogs have been evaluated for anti-inflammatory potential, followed by subsequent *in silico* analyses in this work.

■ EXPERIMENTAL SECTION

Materials

Necessary reagents and chemicals have been collected from TCI (India), TCI (Japan) and Sigma-Aldrich (USA). Commonly used solvents, like acetone, *n*-hexane, ethanol, methanol, tetrahydrofuran, and dichloromethane were collected from Duksan Pure Chemicals Co. Ltd (South Korea) and Daejung Chemicals & Metals Co. Ltd. (South Korea).

Instrumentation

Nuclear magnetic resonance (NMR) spectra were recorded using Bruker present in Bangladesh Council of Scientific and Industrial Research (BCSIR), Dhaka, Bangladesh. Reference materials were collected from ACI Pharmaceuticals Ltd. (Bangladesh). The reaction progress was monitored by analytical thin layer chromatography pre-coated silica gel plates (0.25 mm 60 F-254) collected from Merck (Germany). The synthesized crude products were purified by flash column chromatography using 200–400 mesh size silica gel.

Procedure

General method for coupling the phenol with alkyl halide

The various phenols were coupled with alkyl bromide by following reported methods [18-19] with minor modifications. Powdered oven-dried potassium carbonate was added to a mixture of substituted phenols in anhydrous solvent (Fig. 2). After stirring for 30 min, methyl bromoacetate was added dropwise, and the mixture was heated at 80 °C for 2–6 h. The reaction progress was monitored by thin-layer chromatography. At the end of the reaction, the solvent was removed by rotary evaporator. Water and ethyl acetate were added to the remaining residue. The resultant organic layer was collected and dried by using anhydrous sodium sulfate.

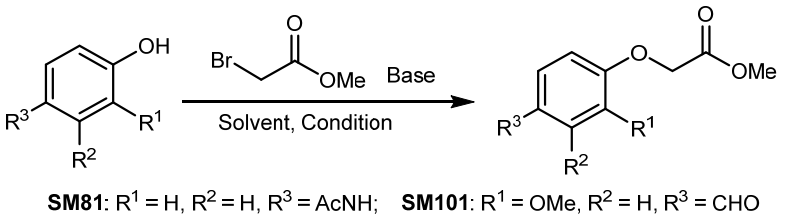

Fig 2. Coupling of phenols with alkyl halide

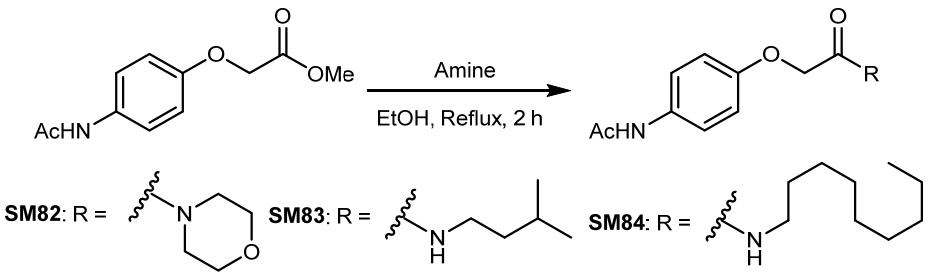

Fig 3. Synthesis of amide from methyl ester

After subsequent filtration, the filtrate was evaporated under vacuum to get the crude product, which was then purified by flash column chromatography to obtain the pure coupled compound.

General method for synthesis of amide from methyl ester

At room temperature, the ester was taken in absolute ethanol in a round bottom flask. With continuous stirring, appropriate amine was added. The final mixture was refluxed for 2 h (Fig. 3). The reaction progress was monitored by using thin-layer chromatography techniques. At the end of the reaction, the solvent was removed by rotary evaporator. Water and ethyl acetate were added to the residue, and the organic layer was collected and dried over anhydrous sodium sulfate. After subsequent filtration, the filtrate was collected and then evaporated under vacuum to get the crude product, which was then purified by flash column chromatography to get the pure amide.

In another attempt, the reaction was tried in solvent-free conditions. The ester was taken in morpholine, and the mixture was triturated in mortar and pestle for 4 h. The progress of the reaction was monitored by thin-layer chromatography. After 4 h, ethyl acetate and water were added to the semisolid residue. The organic layer was collected, dried over anhydrous sodium sulfate, and filtered. The filtrate was evaporated under rotary to get the crude mass, which was purified by flash column chromatography to obtain the pure coupled compound.

General method for the synthesis of amide from acid

The appropriate acid was taken in a round bottom flask, and thionyl chloride was added to the flask at room temperature [20]. The mixture was then refluxed for 2 h (Fig. 4), during which gas generation was ceased. Thin layer chromatography techniques were applied to check the progress of the reactions. As the monitoring technique, a drop of the mixture was added to a small amount of dry methanol, and then the presence of methyl ester along with acid was observed. At the end of acyl chloride formation, the excess thionyl chloride was removed by dry toluene co-evaporation. Dry dichloromethane and triethylamine were added to the residue under the ice bath system. The amine was added and the mixture was allowed to warm to room temperature. Stirring was continued overnight. At the end of the reaction, the solvent was removed by a vacuum applied by a rotary evaporator. Water and ethyl acetate were added to the resulting residue. The organic layer was collected, dried over anhydrous sodium sulfate, and filtered. The filtrate was evaporated under the rotary to get the crude product, which was purified by flash column chromatography to obtain the pure amide.

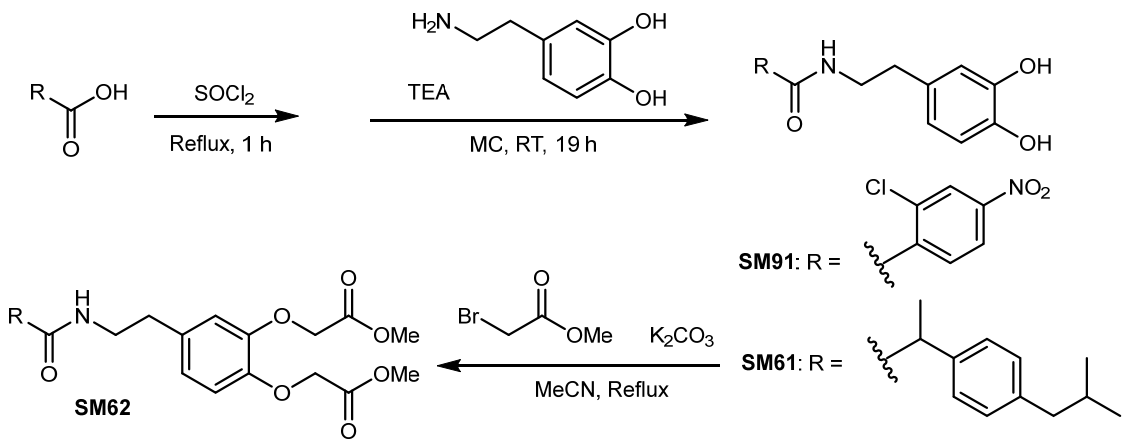

Fig 4. Synthesis of amides from acids

Analgesic activity by writhing test in mice

Reported method [21] with minor modification was used for these *in vivo* observations. Swiss albino mice were taken in groups of 6 animals each for the test, standard, and controls. The test groups were given compound doses of 5, 10, 20, and 40 mg/kg of body weight. Similarly, diclofenac sodium was given at a standard dose of 0.5 mg/kg, and normal saline was given in the control groups. The mice were given the test compounds and standards orally 30 min before the administration of 0.7% (v/v) acetic acid (0.01 mL/g) intraperitoneally. The number of writhing (abdominal constrictions) was counted for 30 min for every group animal. The percentage of protection was done using the formula in Eq. (1).

$$\%\,\text{Protection} = 100\times\left(1-\frac{\text{No. of writhing in sample}}{\text{No. of writhing in control}}\right) \quad (1)$$

In vitro *anti-inflammatory activity by inhibition of egg albumin denaturation*

Reported method [22] with minor modifications was applied for this study. Here, 0.2 mL of egg albumin was taken, and 2.8 mL of phosphate buffer saline of pH 6.4 was added. Subsequently, 2 mL of varying concentrations of test compounds were added to the mixtures. Similar mixtures were made by replacing the test compound with ibuprofen to get the positive controls. Similarly, the phosphate buffer solution, without test compounds, was considered the negative control. Denaturation observed from these blank solutions was considered as 100%. The resultant mixtures were incubated at 37 °C for 15 min and then heated at 70 °C for another 5 min. After cooling the mixtures under tap water, absorbance values were recorded at 660 nm. The percentage inhibition of denaturation was calculated by following the formula in Eq. (2);

$$\%\text{Inhibition of Inflammation} = 100\times\left(\frac{\text{OD2}-\text{OD1}}{\text{OD2}}\right) \quad (2)$$

where, OD1 = absorbance of the test sample and OD2 = absorbance of the control.

In vitro *anti-inflammatory activity by red blood cell membrane stabilization*

Preparation of suspension of red blood cells (RBC). Fresh whole human blood (10 mL) was mixed with heparin in the centrifuge tube. The mixture was then centrifuged for 10 min at 3000 rpm. Subsequently, the supernatant was discarded, and the residue was washed with an equal volume of normal saline three times. The residual blood was reconstituted as 10% v/v RBC suspension with normal saline for the following applications.

Observation of stabilization against heat induced hemolysis. Membrane stabilization was checked by following the reported method [23] with minor modifications. Isotonic buffer solution (5 mL each) was taken in centrifuge tubes having 50, 100, 200 and 400 µg/mL of test drugs. The experiments were run by taking 6 sets for each concentration. Tubes with 5 mL of vehicle were taken as a negative control. Diclofenac was taken as the reference standard. To each of the centrifuge tubes, 0.05 mL of RBC suspensions were added. After gentle mixing, one set of the various types of tubes were

incubated at 54 °C for 20 min, and the remaining sets were maintained at 0-4 °C for 20 min. After heating the centrifuge tubes were cooled, and the reaction mixtures were centrifuged at 3,000 rpm for 3 min. The supernatants were observed for absorbance (OD) at 540 nm using isotonic buffer solution as the blank. Analysis was done by the following Eq. (3);

$$\%\text{Inhibition of hemolysis} = 100 \times \left(1 - \frac{OD2 - OD1}{OD3 - OD1}\right) \quad (3)$$

where OD1 = absorbance of the unheated test sample, OD2 = absorbance of the heated test sample, and OD3 = absorbance of the control sample heated.

Observation of in vivo *anti-inflammatory activity in mice*

The compounds were also evaluated for their anti-inflammatory activity in the mice model. As the method development plan, the Swiss Albino mice were selected and maintained in the laboratory for 3 d. Then, for analysis, 0.2 mL of acetic acid (1% v/v) was administered in mice by intraperitoneal injection. A digital vernier scale measured the thickness of the mice leg paw at 0, 30, 60, 90, and 120 min intervals. During the development of this method, diclofenac was administered immediately after administration of the acetic acid, and this group was considered as the reference group. The same measurement was made by taking mice groups and administering the vehicles only, which was regarded as the blank.

Observation by this method was positive, where there was an obvious correlation with the administration of positive control. This group had clearly reduced diameter, as observed in the method development procedure. Then, the test compounds were subjected to the same procedure to observe the reduction of inflammation for this observation. To find out the inflammation, the following formula was followed in Eq. (4);

$$\%\text{Inflammation}\left(I_x\right) = 100 \times \left(\frac{D_T - D_0}{D_0}\right) \quad (4)$$

where D_T = Paw thickness at time T, D_0 = Paw thickness at zero time. The reduction of inflammation is calculated using Eq. (5);

$$\text{Reduction of inflammation} = I_b - I_s \quad (5)$$

where, I_b = Inflammation in blank at time T, I_s = Inflammation in sample at time T.

In silico *analysis*

Protein preparation. The published [24] PDB entry 4PH9, having Ibuprofen as the ligand, was chosen for this study. This ligand and other heteroatoms were first removed by using Notepad editor to get the free protein molecule, which was then converted to the corresponding PDBQT format using the Autodock Tools (version-1.5.6). Similarly, structures of the synthesized compounds drawn by ChemDraw (Version 12.0) were converted to the corresponding PDBQT files and then were taken for docking [25] by Autodock Vina (version-1.1.2).

Ligand preparation. The structures of the desired molecules were first drawn in ChemDraw (version-12.0). Subsequently, these structures were saved as PDB files. In the final stage the PDB structures were saved as the PDBQT file necessary for docking with the Autodock Vina.

Docking by using Autodock Vina. Docking analysis was done by using Autodock Vina to predict the protein-ligand interactions. The 4PH9 file was published with its own ligand; thus, the pocket occupied by this ligand was taken as the binding site. The conformations with the lowest energy (highest affinities) were considered for analyzing the binding interactions.

In silico *pharmacokinetic profiling*

In silico pharmacokinetic analysis was done by using pkCSM software [26-27]. For this study, the structures were converted to the SMILES format using the www.cheminfo.org online SMILES generator. The reported [27-28] Lipinski's rule of 5' and PAINS filter [29] were adopted to find out the drug-likeness of the compounds under study. These rules are still widely used to predict the likelihood that any given compound will be orally active. This guideline from Lipinski considers compounds are more likely to have drug-likeness if they have optimum values in some predictive features (molecular weight < 500 Daltons, clogP < 5, hydrogen bond donors ≤ 5, hydrogen bond acceptors ≤ 10). The PAINS filter additionally considers some other predictable features (number of freely rotatable bonds ≤ 10, number of chiral center ≤ 3, average polar surface area ≅ 67).

■ RESULTS AND DISCUSSION

Synthesis of the Compounds

Variable yields were obtained in this study by coupling phenols with the alkyl halides (Table 1). Acetonitrile gave 81–89% yield and thus was better as the solvent than DMF. However, moderate to excellent yields were found in these reactions. While trying amide coupling, yields were good to excellent (79–89%) (Table 2).

Characterization of Synthesized Compounds

For characterization of the compounds, ^{1}H NMR spectra were recorded on Bruker at 600 MHz. Chemical shifts have been quoted in parts per million (ppm) referenced to the solvent peak or 0.0 ppm for tetramethyl silane (TMS). The peak splitting patterns were described as: br = broad, s = singlet, d = doublet, t = triplet, q = quartet and m = multiplet. Coupling constants, *J*, were reported in hertz unit (Hz). ^{13}C-NMR spectra were recorded at 151 MHz and fully decoupled by broad band proton decoupling. Chemical shifts have been mentioned in ppm referenced to the center of a triplet at 77.0 ppm of $CDCl_3$ or appropriate solvent peaks. However, the observed values have been discussed in the following section:

***N*-(3,4-dihydroxyphenethyl)-2-(4-isobutylphenyl)propanamide (SM61):** ^{1}H-NMR (600 MHz, $CDCl_3$): δ = 0.83 (d, *J* = 6.0 Hz, 6H), 1.42 (d, *J* = 12.0, 3H), 1.75–1.81 (m, 1H), 2.39 (d, *J* = 6.0 Hz, 2H), 2.51 (t, *J* = 6.0 Hz, 2H), 3.26–3.32 (m, 1H), 3.34–3.39 (m, 1H), 3.44 (q, *J* = 6.0 Hz, 1H), 5.42–5.44 (m, 1H), 6.32–6.33 (m, 1H), 6.53 (d, *J* = 6.0 Hz, 1H), 6.67 (d, *J* = 6.0 Hz, 1H), 7.03 (m, 4H) ppm. ^{13}C-NMR (151 MHz, $CDCl_3$): δ = 18.14, 22.39, 30.17, 34.71, 41.10, 45.00, 46.69, 115.14, 115.51, 120.49, 127.43, 129.74, 130.37, 137.55, 141.07, 143.13, 144.21, 175.86 ppm. The HRMS spectrum showed the mass as 342.2072 $(M+H)^+$, consistent with the calculated exact mass 341.1991.

Table 1. Condition optimization for coupling of phenols with alkyl halide

Sl.	Solvent	Base	Temperature (°C)	Time (h)	Yield (%)
1	DMF	K_2CO_3	90	2	65–83
2	Acetonitrile	K_2CO_3	80	2	78–92
3	Acetonitrile	K_2CO_3	80	6	81–89

Table 2. Synthesis of amide from methyl ester

Sl.	Solvent	Amine	Condition	Time (h)	Yield (%)
1	Ethanol	Morpholine	Reflux	2	89
2	Ethanol	Isoamylamine	Reflux	2	85
3	Ethanol	Nonylamine	Reflux	2	79
4	--	Morpholine	25 °C	4	81

Dimethyl-2,2'-((4-(2-(2-(4-isobutylphenyl)propanamido)ethyl)-1,2-phenylene)bis(oxy)) diacetate (SM62): ^{1}H-NMR (600 MHz, $CDCl_3$): δ = 0.83 (d, *J* = 6.0 Hz, 6H), 1.41 (d, *J* = 12.0, 3H), 1.76–1.80 (m, 1H), 2.39 (d, *J* = 12.0 Hz, 2H), 2.54–2.57 (m, 2H), 3.27–3.34 (m, 2H), 3.35–3.42 (m, 1H), 3.73 (s, 6H), 4.62 (s, 4H), 5.27–5.29 (m, 1H), 6.49–6.50 (m, 1H), 6.57 (s, 1H), 6.67 (d, *J* = 6.0 Hz, 1H), 7.02–7.06 (m, 4H) ppm. ^{13}C-NMR (151 MHz, DMSO-d_6): δ = 18.97, 22.64, 30.09, 34.89, 44.71, 45.16, 52.20, 52.22, 65.85, 66.00, 114.96, 115.48, 122.17, 127.41, 129.17, 133.64, 139.61, 139.99, 146.10, 147.53, 169.73, 169.84, 173.76 ppm. The HRMS spectrum showed the mass as 486.2506 $(M+H)^+$, consistent with the calculated exact mass 485.2414.

Methyl 2-(4-acetamidophenoxy)acetate (SM81): ^{1}H-NMR (600 MHz, $CDCl_3$): δ = 2.08 (s, 3H), 3.73 (s, 3H), 4.54 (s, 2H), 6.79 (d, *J* = 12.0 Hz, 2H), 7.33 (d, *J* = 12.0 Hz, 2H) ppm. ^{13}C-NMR (151 MHz, $CDCl_3$): δ = 24.27, 52.30, 65.64, 115.02, 121.88, 132.10, 154.50, 168.53, 169.48 ppm. The HRMS spectrum showed the mass as 224.0924 $(M+H)^+$, consistent with the calculated exact mass 223.0845.

***N*-(4-(2-Morpholino-2-oxoethoxy)phenyl)acetamide (SM82):** ^{1}H-NMR (600 MHz, $CDCl_3$): δ = 2.08 (s, 3H), 3.53–3.60 (m, 8H), 4.60 (s, 2H), 6.82 (d, *J* = 12.0 Hz, 2H), 7.31–7.34 (m, 3H) ppm. ^{13}C-NMR (151 MHz, $CDCl_3$): δ = 24.24, 42.46, 45.89, 66.72, 66.79, 67.81, 114.90, 121.97, 132.13, 154.40, 166.67, 168.56 ppm. The HRMS spectrum showed the mass as 279.1345 $(M+H)^+$, consistent with the calculated exact mass 278.1267.

2-(4-Acetamidophenoxy)-*N*-isopentylacetamide (SM83): ^{1}H-NMR (600 MHz, $CDCl_3$): δ = 0.86 (d, *J* = 6.0 Hz, 6H), 1.35–1.39 (m, 2H), 1.53–1.55 (m, 1H), 2.10 (s, 3H), 3.27–3.31 (m, 2H), 4.38 (s, 2H), 6.45 (br, 1H), 6.81 (d, *J* = 6.0 Hz, 2H), 7.05 (br, 1H), 7.37 (d, *J* = 6.0 Hz, 2H)

ppm. ^{13}C-NMR (151 MHz, $CDCl_3$): δ = 22.41, 24.24, 25.97, 37.44, 38.33, 67.71, 115.02, 121.98, 132.47, 153.89, 168.14, 168.64 ppm. The HRMS spectrum showed the mass as 279.1708 $(M+H)^+$, consistent with the calculated exact mass 278.1630.

2-(4-Acetamidophenoxy)-*N*-nonylacetamide (SM84): ^{1}H-NMR (600 MHz, $CDCl_3$): δ = 0.81 (t, *J* = 6.0 Hz, 3H), 1.19–1.23 (m, 12H), 1.45–1.48 (m, 2H), 2.10 (s, 3H), 3.24–3.28 (m, 2H), 4.38 (s, 2H), 6.49 (br, 1H), 6.81 (d, *J* = 6.0 Hz, 2H), 7.18 (br, 1H), 7.37 (d, *J* = 6.0 Hz, 2H) ppm. ^{13}C-NMR (151 MHz, $CDCl_3$): δ = 14.11, 22.66, 24.34, 26.86, 29.23, 29.25, 29.47, 29.53, 31.85, 39.13, 67.72, 115.03, 121.92, 132.46, 153.88, 168.11, 168.44 ppm. The HRMS spectrum showed the mass as 335.2334 $(M+H)^+$, consistent with the calculated exact mass 334.2256.

2-Chloro-*N*-(3,4-dihydroxyphenethyl)-4-nitrobenzamide (SM91): ^{1}H-NMR (600 MHz, $CDCl_3$): δ = 2.79 (t, *J* = 6.0 Hz, 2H), 3.64–3.68 (m, 2H), 6.09 (br, 1H), 6.57–6.59 (m, 1H), 6.71 (d, *J* = 1.98 Hz, 1H), 6.74 (d, *J* = 6.0 Hz, 1H), 7.64 (d, *J* = 6.0 Hz, 1H), 8.06-8.08 (m, 1H), 8.18 (d, *J* = 2.16 Hz, 1H) ppm. ^{13}C-NMR (151 MHz, $CDCl_3$): δ = 34.78, 41.44, 115.97, 116.53, 119.79, 122.75, 124.97, 130.30, 130.33, 131.50, 143.26, 144.08, 145.55, 148.54, 165.18 ppm. The HRMS spectrum showed the mass as 337.0592 $(M+H)^+$, consistent with the calculated exact mass 336.0513.

Methyl 2-(4-formyl-2-methoxyphenoxy)acetate (SM101): ^{1}H-NMR (600 MHz, $CDCl_3$): δ = 3.75 (s, 3H), 3.89 (s, 3H), 7.73 (s, 2H), 6.82 (d, *J* = 6.0 Hz, 1H), 7.35–7.38 (m, 2H), 9.80 (s, 1H) ppm. ^{13}C-NMR (151 MHz, $CDCl_3$): δ = 52.47, 56.10, 65.84, 109.87, 112.32, 126.16, 131.21, 149.97, 152.43, 168.53, 190.84 ppm. The HRMS spectrum showed the mass as 225.0764 $(M+H)^+$, consistent with the calculated exact mass 224.0685.

In Vitro Anti-inflammatory Activity by Inhibition of the Egg Albumin Denaturation

All compounds had dose-dependent activity while considering the inhibition of egg albumin denaturation (Fig. 5). However, compounds like **SM83** and **SM101** were

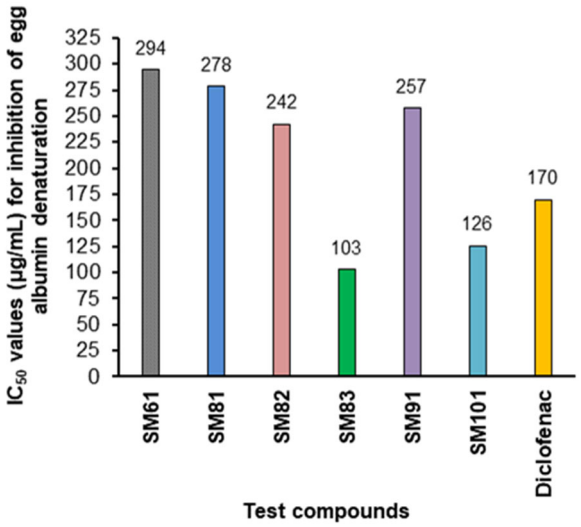

Fig 6. Calculated IC_{50} values for reduction of egg albumin denaturation

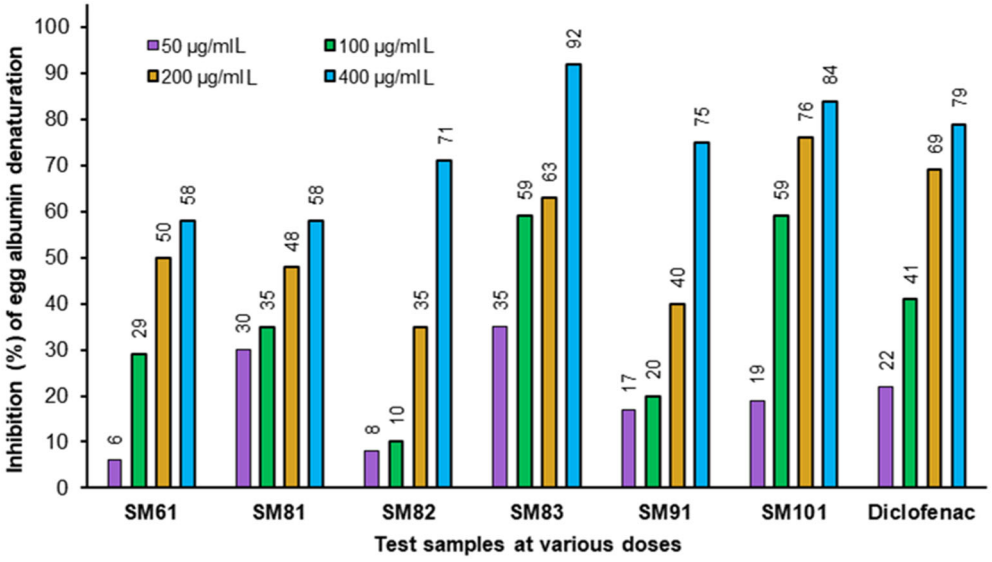

Fig 5. Inhibition (%) of denaturation of egg albumin

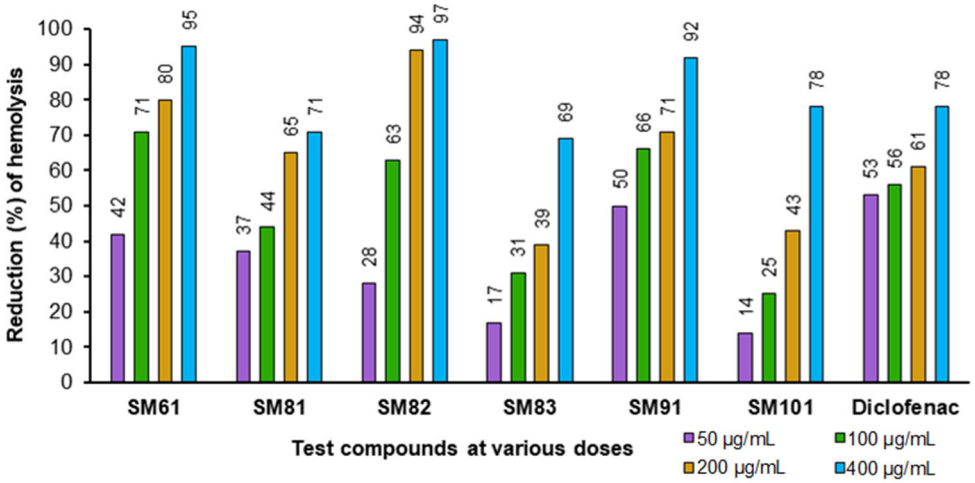

Fig 7. Reduction of lysis of human red blood cells

more powerful inhibitors against egg albumin denaturation. The amides, **SM82** and **SM83**, were more robust when compared with the corresponding ester, **SM81**. The observations were taken for calculating the IC_{50} values for inhibition of egg albumin denaturation (Fig. 6). Compound **SM83** offered the lowest IC_{50} values (103 µg/mL) in this study, whereas the second most potent compound was **SM101** (IC_{50} = 126 µg/mL).

In Vitro Anti-inflammatory Activity by Stabilization of Human Red Blood Cell Membrane

By considering the inhibition of hemolysis (Fig. 7), there was dose-dependent activity from all of the synthesized compounds. In this case, the potent compounds were **SM61**, **SM82**, and **SM91**. The amide, **SM82**, was more powerful than the corresponding ester, **SM81**. The observations from human RBC membrane stabilization were taken to calculate the IC_{50} values for the inhibition of hemolysis. Compounds **SM61**, **SM82**, and **SM91** gave the lowest IC_{50} values (15.7, 69.0, and 5.3 µg/mL, respectively) in this study (Fig. 8).

Observation of *In Vivo* Anti-inflammatory activity

The anti-inflammatory activity was observed by applying a simple method using a mice model with some selected compounds based on the results obtained from the *in vitro* anti-inflammatory assay methods as well as the *in vivo* analgesic activity study. While comparing the inhibitions, as measured by comparing the inflammations

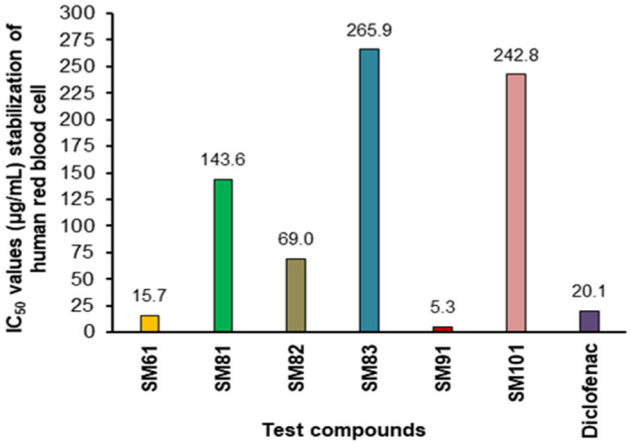

Fig 8. Calculated IC_{50} values for stabilization of human red blood cell

from the blank at the same time, most of the compounds were comparable with the standard diclofenac (Fig. 9 and 10). Even **SM83**, **SM91**, and **SM101** were relatively more potent in this study.

In Silico Studies with the Synthesized Compound

However, after getting excellent results from the *in vitro* and *in vivo* experiments, some of the potent compounds (**SM61**, **SM81**, **SM82**, and **SM83**) were taken for the molecular docking in the binding site of COX-2 enzyme. The collected PDB (ID: 4PH9) contained ibuprofen as the ligand. Therefore, the outputs from docking in this enzyme were overlapped with the reported ligand for predicting the binding patterns.

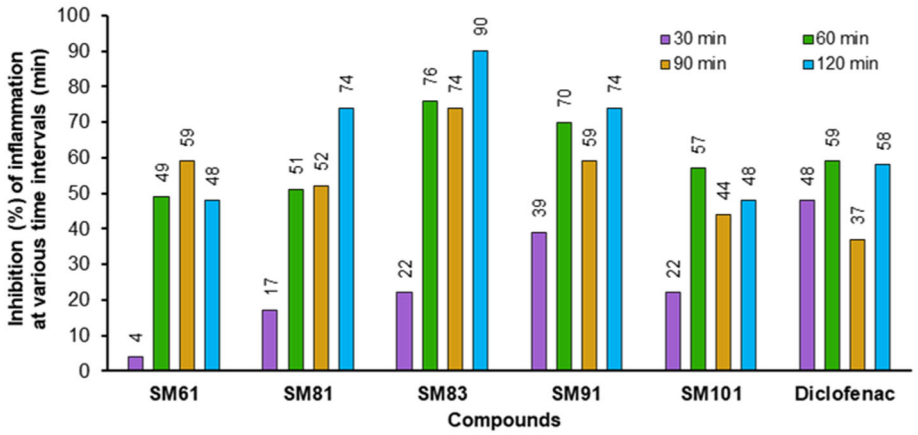

Fig 9. Inhibition (%) of inflammation at various time intervals after 10 mg/kg dose

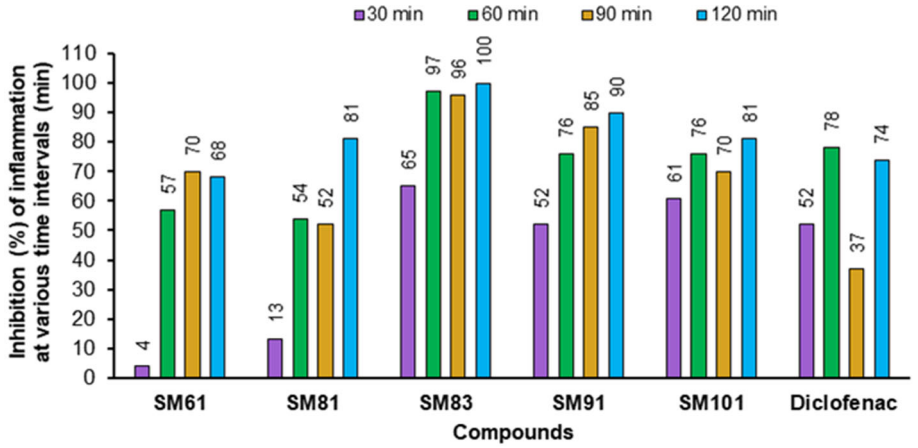

Fig 10. Inhibition (%) of inflammation at various time intervals after 20 mg/kg dose

For running the docking operations, the center (x,y,z = 13.5,23.5,25.0), as well as pocket size (x,y,z = 12,10,8), were predicted according to Autodock Vina by observing the reported orientation of ibuprofen. The binding affinities were recorded for each of the orientations after docking activities. The values are presented in Table 3. The lowest energy modes were taken for comparative analysis with ibuprofen.

The observed activity of compound **SM61** was analyzed for correlations with the binding patterns. While comparing with the reported orientation of ibuprofen in the binding site of COX enzyme, the test compound (**SM61**) got a similar orientation as shown in Fig. 11. The residues with polar extensions, like, TYR356 and TYR386 seem to get polar interactions with the ligand. However, the excess length of **SM61** appears to have a negative effect on the binding potential, thereby offering lesser inhibitory potential as observed from the writhing inhibition study.

Table 3. Binding affinity of potent compounds

Modes found	Binding affinity (kcal/mol) of compounds			
	SM61	**SM81**	**SM82**	**SM83**
1	−7.4	−7.2	−6.7	−6.7
2	−6.1	−6.9	−6.7	−6.5
3	−6.0	−6.9	−6.7	−6.3
4	−6.0	−6.5	−6.6	−6.2
5	−5.0	−6.2	−6.6	−6.0
6	−4.6	−6.1	−6.5	−5.6
7	−4.5	−5.8	−6.3	−5.1
8	-	−5.6	−6.2	−5.0
9	-	−4.9	−6.1	−4.9

Compound **SM81** also had an orientation similar to ibuprofen, as shown in Fig. 12. The residues TYR356, GLY527, and ALA528 might have essential roles in the enzyme's binding site. TYR386 also seems to have roles in

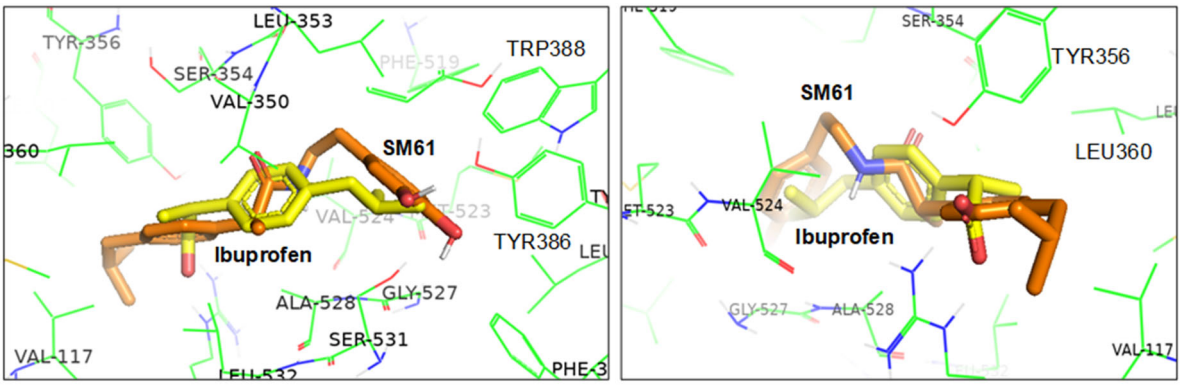

Fig 11. Orientation of **SM61** and ibuprofen (yellow) in the binding site of COX-2 enzyme (Two different views)

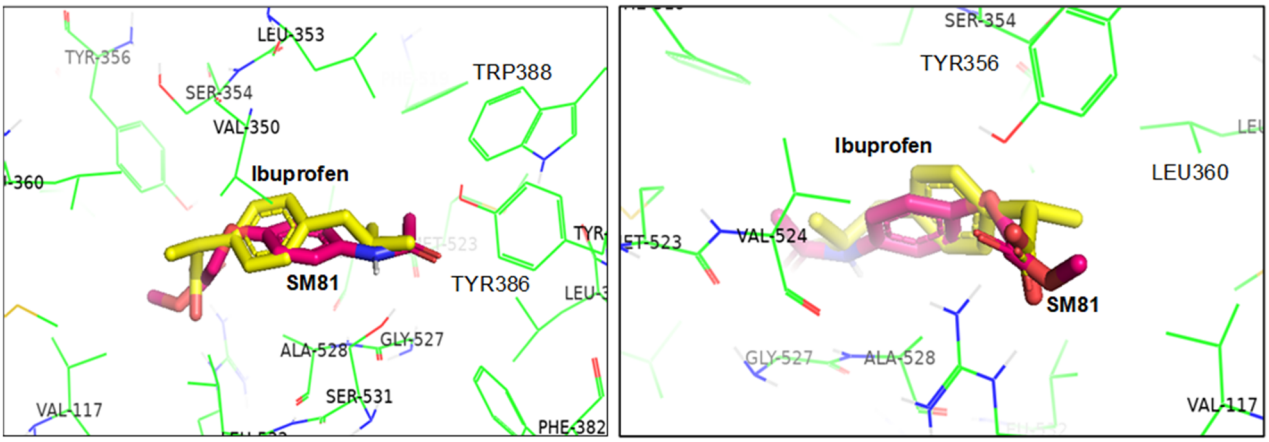

Fig 12. Orientation of **SM81** and ibuprofen (yellow) in the binding site of COX-2 enzyme (Two different views)

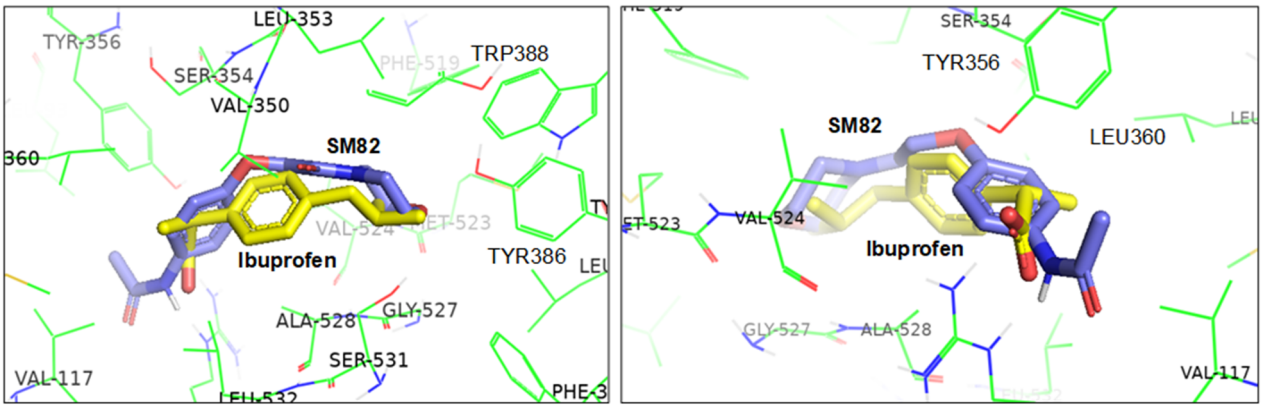

Fig 13. Orientation of **SM82** and ibuprofen (yellow) in the binding site of COX-2 enzyme (Two different views)

binding the compound **SM81** to the binding site of the COX-2 enzyme. The orientation of **SM82** was also similar in the binding site of the COX enzyme, as shown in Fig. 13. However, the additional morpholine group of **SM82** pushed the acetamide group closer to the VAL117 residue itself close to VAL524, thereby increasing the binding interaction with the pocket, resulting in lower IC_{50} values. While observing the orientation of **SM83**, the findings were similar to that of **SM82**, as shown in Fig. 14. Here, TYR356 and VAL350 might have particular interactions of the ligand with the binding site of the COX-2 enzyme.

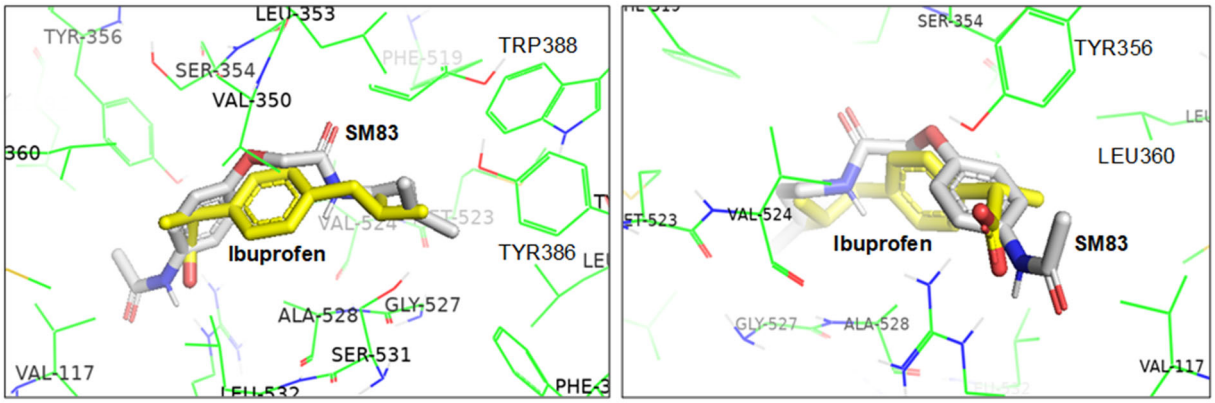

Fig 14. Orientation of **SM83** and ibuprofen (yellow) in the binding site of COX-2 enzyme (Two different views)

In Silico Pharmacokinetic Profiling

From Lipinski's rule for predictive features (molecular weight < 500 Daltons, clogP < 5, hydrogen bond donor ≤ 5, hydrogen bond acceptor ≤ 10), it should be noted that all compounds have optimal drug similarity, as shown in Table 4. All of the compounds had the drug-likeness property after overall consideration. Though **SM62** and **SM84** had rotatable bonds beyond the optimum value, they have all the other values within the desired range. However, these two compounds were of a little interesting because of their comparatively lower anti-inflammatory potential. The compounds had optimum values for most features while observing the absorption and distribution of the pharmacokinetic properties (Table 5). Only a few cases were the exceptions, including **SM62** and **SM84**. Interestingly, these were again the same compounds with lower anti-inflammatory potentials.

Table 4. PAINS filter and Lipinski's rule of five for drug-likeness of the synthesized compounds

Compound	Hydrogen bond acceptors	Hydrogen bond donors	Consensus Log $P_{o/w}$	Molecular weight	No. of Rotatable bonds	No. of rings	Polar surface area	Drug-likeness
Accepted range	≤ 10	≤ 5	< 5	< 500	< 10	1–4	67	
SM61	3	3	4.745	339.47	8	2	69.56	Yes
SM62	7	1	4.110	485.57	16	2	100.16	Yes
SM81	4	1	1.196	223.23	4	1	64.63	Yes
SM82	4	1	0.882	278.31	6	2	67.87	Yes
SM83	3	2	2.186	278.35	9	1	67.43	Yes
SM84	3	2	3.890	334.46	14	1	67.43	Yes
SM91	5	3	2.631	336.73	6	2	115.38	Yes
SM101	5	0	2.003	236.27	6	1	61.83	Yes

Table 5. Pharmacokinetic properties in terms of absorption and distribution

		Predicted values from absorption study by pkCSM							Predicted values from distribution study			
SI	Compound	Water solubility	$CaCo_2$ permeability	Intestinal absorption (human)	Skin permeability	P-gp substrate	P-gp I inhibitor	P-gp II inhibitor	VDss (human)	Fraction unbound (human)	BBB permeability	CNS permeability
		(log mol/L)	(log Papp in 10^{-6} cm/s)	(%) Absorbed	(log Kp)	(Yes/No)	(Yes/No)	(Yes/No)	(log L/kg)	(Fu)	(log BB)	(log PS)
1	**SM61**	−3.954	1.129	91.171	−2.864	Yes	Yes	No	0.313	0.127	−0.668	−2.360
2	**SM62**	−6.069	0.436	77.799	−2.759	Yes	Yes	Yes	−0.086	0	−1.015	−3.269
3	**SM81**	−2.143	0.344	83.045	−3.097	No	No	No	−0.314	0.467	−0.226	−2.954

SI	Compound	Predicted values from absorption study by pkCSM							Predicted values from distribution study			
		Water solubility	$CaCo_2$ permeability	Intestinal absorption (human)	Skin permeability	P-gp substrate	P-gp I inhibitor	P-gp II inhibitor	VDss (human)	Fraction unbound (human)	BBB permeability	CNS permeability
		(log mol/L)	(log Papp in 10^{-6} cm/s)	(%) Absorbed	(log Kp)	(Yes/No)	(Yes/No)	(Yes/No)	(log L/kg)	(Fu)	(log BB)	(log PS)
4	**SM82**	−2.510	0.651	80.826	−3.227	No	No	No	−0.267	0.458	−0.379	−2.979
5	**SM83**	−2.972	0.896	90.964	−2.778	Yes	No	No	−0.121	0.306	−0.010	−2.625
6	**SM84**	−4.124	0.804	89.108	−2.737	Yes	Yes	No	0.139	0.175	−0.178	−2.702
7	**SM91**	−4.082	0.105	78.486	−2.811	Yes	No	No	−0.155	0.083	−0.923	−2.471
8	**SM101**	−2.204	1.232	89.776	−2.581	No	No	No	−0.321	0.442	−0.186	−2.894

Table 6. Pharmacokinetic properties in terms of metabolism and excretion

SI	Compound	Predicted values from metabolism study by pkCSM							Excretion study	
		CYP2D6 substrate	CYP3A4 substrate	CYP1A2 inhibitor	CYP2C19 inhibitor	CYP2C9 inhibitor	CYP2D6 inhibitor	CYP3A4 inhibitor	Total clearance	Renal OCT2 substrate
		(Yes/No)	(Yes/No)	(Yes/No)	(Yes/No)	(Yes/No)	(Yes/No)	(Yes/No)	(log mL/min/kg)	(Yes/No)
1	**SM61**	No	No	Yes	Yes	Yes	No	Yes	0.246	No
2	**SM62**	No	Yes	No	Yes	Yes	No	Yes	0.628	No
3	**SM81**	No	No	No	No	No	No	No	0.672	No
4	**SM82**	No	No	No	No	No	No	No	0.524	No
5	**SM83**	No	No	No	No	No	No	No	0.382	No
6	**SM84**	No	No	No	Yes	Yes	No	No	1.495	No
7	**SM91**	No	Yes	Yes	Yes	Yes	No	No	0.093	No
8	**SM101**	No	No	No	No	No	No	No	0.808	No

Table 7. Pharmacokinetic properties in terms of toxicity

SI	Compound	Predicted values from toxicity study by pkCSM							
		AMES toxicity	Max. tolerated dose (human)	hERG I inhibitor	hERG II inhibitor	Oral rat acute toxicity LD_{50})	Oral rat chronic toxicity (LOAEL)	Hepatotoxicity	Skin Sensitization
		(Yes/No)	(log mg/kg/day)	(Yes/No)	(Yes/No)	(mol/kg)	(log mg/kg/day)	(Yes/No)	(Yes/No)
1	**SM61**	No	0.384	No	Yes	1.975	1.675	Yes	No
2	**SM62**	No	0.722	No	No	1.74	2.491	Yes	No
3	**SM81**	No	1.036	No	No	2.221	1.520	No	No
4	**SM82**	No	0.207	No	No	2.688	0.886	No	No
5	**SM83**	No	−0.027	No	No	2.332	1.376	No	No
6	**SM84**	No	−0.461	No	Yes	2.624	1.171	Yes	Yes
7	**SM91**	Yes	−0.086	No	No	2.88	2.255	No	No
8	**SM101**	No	1.596	No	No	2.06	2.100	No	No

The metabolism and excretion data, as shown in Table 6, were also within the acceptable range. However, some random data were slightly beyond the acceptable range. Thus, the scaffolds were found to have the optimum pharmacokinetic properties. The toxicity data were also observed in this project work. While running the pkCSM program for predicting the toxicity profile, the synthesized compounds exhibited little to no toxicity likelihood as shown in Table 7. Thus, the scaffolds were found to possess a good safety profile.

■ CONCLUSION

This study has compared several 2-phenoxy acetic acid analogs for their anti-inflammatory potential. The compounds were achieved by some simple high-yield coupling reactions. In both the *in vitro* and *in vivo*

studies, the compounds were potent as anti-inflammatory agents. There was dose-dependent anti-inflammatory activity, and the observations were more or less similar in both *in vitro* and *in vivo* studies. Some esters and corresponding amides showed the most potent anti-inflammatory activity. While observing the orientations and the binding interactions in the binding site of the COX-2 enzyme, the compounds were getting orientations similar to that of the reported standard, ibuprofen. Thus, these scaffolds appear to be exciting pharmacophores and can be considered for further derivatizations and exploration.

■ ACKNOWLEDGMENTS

The authors are highly thankful to the Jagannath University and the University of Information Technology and Sciences, Dhaka, Bangladesh, for providing the necessary research facility in the Department of Pharmacy. At the same time, the authors are also grateful to ACI Pharmaceuticals (Ltd.) in Bangladesh for providing the required reference compounds for running this project.

■ CONFLICT OF INTEREST

The authors declare that they have no known conflict of interest that could have appeared to influence the work reported in this paper.

■ AUTHOR CONTRIBUTIONS

Md. Mofazzal Hossain conducted laboratory synthesis and biological experimental procedures and organized the resultant data. Bishyajit Kumar Biswas contributed for conducting synthetic methods and related workup and purification processes. Sukumar Bepary gave this project's main idea, including the synthesis route, necessary characterization methods, and the biological evaluation processes. Sukumar Bepary prepared this manuscript after coordinating the overall laboratory work and writing in detail. All authors agreed to the final version of this manuscript.

■ REFERENCES

[1] Netea, M.G., Balkwill, F., Chonchol, M., Cominelli, F., Donath, M.Y., Giamarellos-Bourboulis, E.J., Golenbock, D., Gresnigt, M.S., Heneka, M.T., Hoffman, H.M., Hotchkiss, R., Joosten, L.A.B., Kastner, D.L., Korte, M., Latz, E., Libby, P., Mandrup-Poulsen, T., Mantovani, A., Mills, K.H.G., Nowak, K.L., O'Neill, L.A., Pickkers, P., van der Poll, T., Ridker, P.M., Schalkwijk, J., Schwartz, D.A., Siegmund, B., Steer, C.J., Tilg, H., van der Meer, J.W.M., van de Veerdonk, F.L., and Dinarello, C.A., 2017, A guiding map for inflammation, *Nat. Immunol.*, 18 (8), 826–831.

[2] Kotas, M.E., and Medzhitov, R., 2015, Homeostasis, inflammation, and disease susceptibility, *Cell*, 160 (5), 816–827.

[3] Furman, D., Campisi, J., Verdin, E., Carrera-Bastos, P., Targ, S., Franceschi, C., Ferrucci, L., Gilroy, D.W., Fasano, A., Miller, G.W., Miller, A.H., Mantovani, A., Weyand, C.M., Barzilai, N., Goronzy, J.J., Rando, T.A., Effros, R.B., Lucia, A., Kleinstreuer, N., and Slavich, G.M., 2019, Chronic inflammation in the etiology of disease across the life span, *Nat. Med.*, 25 (12), 1822–1832.

[4] Malyszko, J., Tesarova, P., Capasso, G., and Capasso, A., 2020, The link between kidney disease and cancer: Complications and treatment, *Lancet*, 396 (10246), 277–287.

[5] Straub, R.H., Cutolo, M., and Pacifici, R., 2015, Evolutionary medicine and bone loss in chronic inflammatory diseases—A theory of inflammation-related osteopenia, *Semin. Arthritis Rheum.*, 45 (2), 220–228.

[6] Straub, R.H., and Schradin, C., 2016, Chronic inflammatory systemic diseases: An evolutionary trade-off between acutely beneficial but chronically harmful programs, *Evol. Med. Public Health*, 2016 (1), 37–51.

[7] Straub, R.H., 2017, The brain and immune system prompt energy shortage in chronic inflammation and ageing, *Nat. Rev. Rheumatol.*, 13 (12), 743–751.

[8] Taniguchi, K., and Karin, M., 2018, NF-κB, inflammation, immunity and cancer: Coming of age, *Nat. Rev. Immunol.*, 18 (5), 309–324.

[9] Verschoor, C.P., Lelic, A., Parsons, R., Evelegh, C., Bramson, J.L., Johnstone, J., Loeb, M.B., and

Bowdish, D.M.E., 2017, Serum C-reactive protein and congestive heart failure as significant predictors of herpes zoster vaccine response in elderly nursing home residents, *J. Infect. Dis.*, 216 (2), 191–197.

[10] GBD 2017 Causes of Death Collaborators, 2018, Global, regional, and national age-sex-specific mortality for 282 causes of death in 195 countries and territories, 1980–2017: A systematic analysis for the Global Burden of Disease Study 2017, *Lancet,* 392 (10159), 1736–1788.

[11] Olvera Alvarez, H.A., Kubzansky, L.D., Campen, M.J., and Slavich, G.M., 2018, Early life stress, air pollution, inflammation, and disease: An integrative review and immunologic model of social-environmental adversity and lifespan health, *Neurosci. Biobehav. Rev.*, 92, 226–242.

[12] Bindu, S., Mazumder, S., and Bandyopadhyay, U., 2020, Non-steroidal anti-inflammatory drugs (NSAIDs) and organ damage: A current perspective, *Biochem. Pharmacol.*, 180, 114147.

[13] Jagannathan, H., Thota, A., Kumarappa, A.K.B., and Kishore, G., 2020, A comparative study of aceclofenac versus etoricoxib in the management of acute low back pain in a tertiary care hospital, *J Drug Assess*., 9 (1), 60–65.

[14] Iolascon, G., Giménez, S., and Mogyorósi, D., 2021, A review of aceclofenac: Analgesic and anti-inflammatory effects on musculoskeletal disorders, *J. Pain Res.,* 14, 3651–3663.

[15] GBD 2016 DALYs and HALE Collaborators, 2017, Global, regional, and national disability-adjusted life-years (DALYs) for 333 diseases and injuries and healthy life expectancy (HALE) for 195 countries and territories, 1990–2016: A systematic analysis for the Global Burden of Disease Study 2016, *Lancet*, 390 (10100), 1260–1344.

[16] Global Burden of Disease Study 2013 Collaborators, 2015, Global, regional, and national incidence, prevalence, and years lived with disability for 301 acute and chronic diseases and injuries in 188 countries, 1990–2013: A systematic analysis for the Global Burden of Disease Study 2013, *Lancet,* 386 (9995), 743–800.

[17] Patel, P.B., and Patel, T.K., 2017, Efficacy and safety of aceclofenac in osteoarthritis: A meta-analysis of randomized controlled trials, *Eur. J. Rheumatol.*, 4 (1), 11–18.

[18] Capelini, C., de Souza, K.R., Barbosa, J.M.C., Salomão, K., Sales Junior, P.A., Murta, S.M.F., Wardell, S.M.S.V., Wardell, J.L., da Silva, E.F., and Carvalho, S.A., 2021, Phenoxyacetohydrazones against *Trypanosoma cruzi*, *Med. Chem. Res.*, 30 (9), 1703–1712.

[19] Díaz-Urrutia, C., Sedai, B., Leckett, K.C., Baker, R.T., and Hanson, S.K., 2016, Aerobic oxidation of 2-phenoxyethanol lignin model compounds using vanadium and copper catalysts, *ACS Sustainable Chem. Eng.*, 4 (11), 6244–6251.

[20] Cloutier, M., Mamone, M., and Paquin, J.F., 2020, Drastic fluorine effect: Complete reversal of the selectivity in the Au-catalyzed hydroalkoxylation reaction of fluorinated haloalkynes, *Chem. Commun.*, 56 (44), 5969–5972.

[21] Thangjam, M.T., Taijong, J., and Kumar, A., 2020, Phytochemical and pharmacological activities of methanol extract of *Artemisia vulgaris* L. leaves, *Clin. Phytosci.*, 6 (1), 72.

[22] Dharmadeva, S., Galgamuwa, L.S., Prasadinie, C., and Kumarasinghe, N., 2018, *In vitro* anti-inflammatory activity of *Ficus racemosa* L. bark using albumin denaturation method, *AYU*, 39, 239–242.

[23] Mahmuda, R., De, T.Q., Shoshi, N.S., Poly, K.A., Saha, P., Bepary, S., Islam, S., and Akhter, S., 2020, *In vitro* anti-inflammatory resorcinol derivatives and their *in silico* analysis, *CTU J. Innovation Sustainable Dev.*, 12 (3), 80–84.

[24] Orlando, B.J., Lucido, M.J., and Malkowski, M.G., 2015, The structure of ibuprofen bound to cyclooxygenase-2, *J. Struct. Biol.*, 189 (1), 62–66.

[25] Trott, O., and Olson, A.J., 2010, AutoDock Vina: Improving the speed and accuracy of docking with a new scoring function, efficient optimization, and multithreading, *J. Comput. Chem.*, 31 (2), 455–461.

[26] Pires, D.E.V., Blundell, T.L., and Ascher, D.B., 2015, pkCSM: Predicting small-molecule pharmacokinetic and toxicity properties using graph-based signatures,

J. Med. Chem., 58 (9), 4066–4072.

[27] Chikowe, I., Bwaila, K.D., Ugbaja, S.C., and Abouzied, A.S., 2024, GC–MS analysis, molecular docking, and pharmacokinetic studies of *Multidentia crassa* extracts' compounds for analgesic and anti-inflammatory activities in dentistry, *Sci. Rep*., 14 (1), 1876.

[28] Mullard, A., 2018, Re-assessing the rule of 5, two decades on, *Nat. Rev. Drug Discovery*, 17 (11), 777.

[29] Baell, J.B., and Holloway, G.A., 2010, New substructure filters for removal of pan assay interference compounds (PAINS) from screening libraries and for their exclusion in bioassays, *J. Med. Chem.*, 53 (7), 2719–2740.